



Path-Constrained Mixture-of-Experts

Zijin Gu, Tatiana Likhomanenko, Vimal Thilak, Jason Ramapuram[†], Navdeep Jaitly[†]

Apple, [†]Google

[†]Work done at Apple.

Sparse Mixture-of-Experts (MoE) architectures enable efficient scaling by activating only a subset of parameters for each input. However, conventional MoE routing selects each layer’s experts independently, creating N^L possible expert paths—for N experts across L layers. This far exceeds typical training set sizes, leading to statistical inefficiency as the model may not learn meaningful structure over such a vast path space. To constrain it, we propose `PathMoE`, which shares router parameters across consecutive layers. Experiments on 0.9B and 16B parameter models demonstrate consistent improvements on perplexity and downstream tasks over independent routing, while eliminating the need for auxiliary load balancing losses. Analysis reveals that tokens following the same path naturally cluster by linguistic function, with `PathMoE` producing more concentrated groups, better cross-layer consistency, and greater robustness to routing perturbations. These results offer a new perspective for understanding MoE architectures through the lens of expert paths.

Correspondence: Zijin Gu: zijin@apple.com

Date: March 20, 2026

1 Introduction

Scaling drives progress in deep learning, but dense models incur computational costs that grow linearly with parameter count. Mixture-of-Experts (MoE) architectures address this by activating only a subset of parameters for each input, decoupling model capacity from computational cost and enabling models with trillions of parameters within practical budgets (Fedus et al., 2022; Jiang et al., 2024).

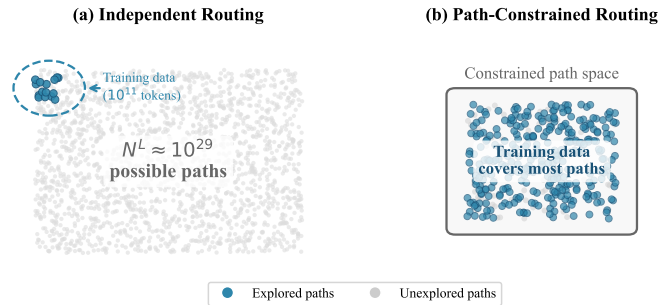


Figure 1 Statistical inefficiency of independent routing.

MoE architectures scale neural networks efficiently by routing each token through a subset of experts at each layer. A token’s journey through an MoE network can be viewed as an *expert path*—a sequence of expert selections (e_1, e_2, \dots, e_L) across L layers (top-1 expert is used). This path perspective reveals a fundamental challenge for conventional MoE routing with independent expert selection at each layer: with N experts per layer, there are N^L possible paths to learn, see Figure 2(a).¹

¹Concretely, a model with 24 layers and 16 experts per layer has $\approx 10^{29}$ possible paths—orders of magnitude larger than the number of tokens reported in typical large model training runs: e.g. a compute-optimal 7B parameter model is trained on $\sim 140\text{B}$ ($\sim 10^{11}$) tokens (Hoffmann et al., 2022). Thus the vast majority of paths receive no learning signal during training.

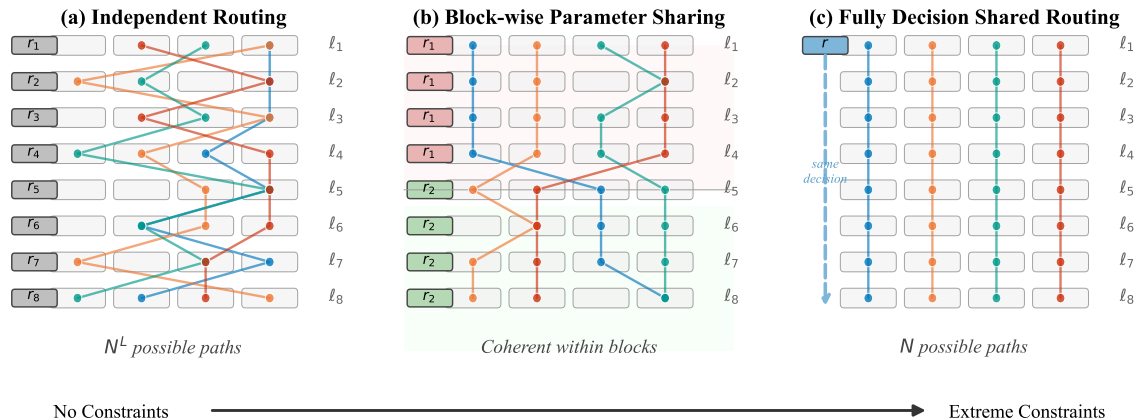


Figure 2 Spectrum of routing constraints in MoE architectures. **(a)** Independent routing: each layer has its own router r_i , creating N^L possible paths for N experts and L layers. **(b)** Block-wise parameter sharing routing, dubbed **PathMoE**: layers within a block share router parameters. **(c)** Fully decision shared routing: all layers share one router and its decision.

This *combinatorial explosion* suggests that conventional MoE routing may be statistically inefficient (Figure 1). Yet these models train well in practice—we find that tokens following the same path naturally cluster by linguistic function, suggesting that emergent structure mitigates the combinatorial challenge. **To further improve sample efficiency and optimization, we argue for constraining the expert path space through architectural design.**

A naive approach is to share routing decisions across all layers (Figure 2(c)), forcing each token to use the same expert throughout the network. This collapses the path space to N paths (linear in the number of experts) but may hurt performance on complex tasks. A more flexible approach is to *share router parameters across all layers*, which does not force identical decisions but encourages consistency through a shared routing function. Recent work has shown this to be effective for speech recognition (Gu et al., 2025), where acoustic features follow structured path patterns.

As text tokens carry more diverse syntactic and semantic patterns than speech frames, different tokens may require fundamentally different processing at different network depths. We thus propose a middle ground: *sharing router parameters across blocks of consecutive layers*, dubbed **PathMoE**, see Figure 2(b). This creates an inductive bias where the same routing function is applied to gradually-evolving token representations within each block. Since nearby layers process similar representations (thanks to residual connections), they naturally receive similar (though not identical) routing—encouraging path coherence without enforcing it, while allowing different blocks to adapt to the changing nature of representations.

We validate **PathMoE** on language modeling and find that it yields key benefits over conventional routing:

1. **Consistent performance gains.** Experiments across 0.9B and 16B parameter models show both improved accuracy on downstream tasks and lower perplexity.
2. **No auxiliary load balancing loss.** **PathMoE** maintains balanced expert utilization without auxiliary losses, eliminating an extra hyperparameter.

Through analysis we further confirm (i) **improved cross-layer coordination**: **PathMoE** achieves 31% higher routing consistency compared to conventional routing; and as a result (ii) **better specialization with greater robustness**: **PathMoE** achieves 11% lower routing entropy while being $22.5\times$ more robust to routing perturbations.

Beyond performance, our expert path view on MoE reveals that paths exhibit interpretable structure: tokens following the same path naturally cluster by linguistic function—punctuation, named entities, temporal expressions—with **PathMoE** producing more concentrated clusters than conventional routing.

2 Related Work

MoE Architectures. The concept of MoE dates back to [Jacobs et al. \(1991\)](#), but has seen renewed interest with the scaling of deep learning models. [Shazeer et al. \(2017\)](#) introduced sparsely-gated MoE layers for neural machine translation, demonstrating that conditional computation could dramatically increase model capacity with modest computational overhead. This work has been extended to large language models with architectures such as Switch Transformers [Fedus et al. \(2022\)](#), GLaM [Du et al. \(2022\)](#), and recently, Mixtral [Jiang et al. \(2024\)](#) and DeepSeek-MoE [Dai et al. \(2024\)](#). While these architectures have demonstrated impressive scaling properties, they all employ independent routing at each layer, treating expert selection as a per-layer decision without considering cross-layer structure.

Routing Mechanisms in MoE. The routing function is critical to MoE performance, determining how inputs are distributed to experts. Classical approaches employ top- k routing with load balancing constraints [Shazeer et al. \(2017\)](#); [Lepikhin et al. \(2020\)](#). Recent work has explored various improvements: [Raposo et al. \(2024\)](#) proposed mixture-of-depths that dynamically adjusts computation depth; [Dai et al. \(2022\)](#) introduced deterministic routing for training stability; [Zhou et al. \(2022\)](#) proposed expert choice routing where experts select tokens; and [Puigcerver et al. \(2023\)](#) investigated soft mixtures that combine all experts with learned weights. These approaches improve individual routing decisions but do not address cross-layer coordination, which we show is critical for expert path efficiency.

Expert Specialization and Redundancy. A growing body of work has investigated what experts learn and whether they develop meaningful specializations. [Chi et al. \(2022\)](#) showed that sparse MoE can suffer from representation collapse where experts learn redundant functions. [Yang et al. \(2024\)](#) proposed compression techniques exploiting inter-expert redundancy. [Zadouri et al. \(2023\)](#) proposed methods to encourage expert diversity through regularization. Our **PathMoE** addresses these concerns architecturally: by encouraging tokens to follow consistent expert paths, experts naturally specialize for different token types without explicit regularization.

Cross-Layer Routing Coordination. While most MoE architectures employ independent routers per layer, recent work has begun exploring cross-layer coordination. [Qiu et al. \(2024\)](#) proposed a recurrent router that conditions each layer’s routing on previous decisions. [Gu et al. \(2025\)](#) demonstrated that sharing router parameters across all layers improves speech recognition, where acoustic features follow structured patterns. Orthogonally, [Dai et al. \(2022\)](#) identified routing fluctuation across training steps and proposed distilling a stable router, addressing temporal rather than spatial coordination. Our **PathMoE** offers a middle ground between independent and fully shared routing: by sharing router parameters within blocks of consecutive layers, we encourage path consistency while allowing adaptation as representations evolve through the network.

3 Methodology

3.1 Preliminaries

MoE Routing. In a transformer model with MoE layers, each MoE layer contains N expert networks $\{F_1, \dots, F_N\}$ and a router r . Given input token representation \mathbf{x} for an MoE layer, the router computes expert probabilities \mathbf{p} :

$$\mathbf{p} = \text{softmax}[r(\mathbf{x})] = \text{softmax}[\mathbf{W}\mathbf{x}], \quad \mathbf{p} \in \mathbb{R}^N. \quad (3.1)$$

Then the output \mathbf{y} is a weighted sum over the top- k experts:

$$\mathbf{y} = \sum_{i \in \text{TopK}(\mathbf{p})} p_i \cdot F_i(\mathbf{x}). \quad (3.2)$$

Let us consider an MoE network with L layers and N experts per layer. For the purpose of analysis we also consider a top-1 expert selection instead of top- k .

Auxiliary Load Balancing Loss. To prevent expert collapse where only a few experts receive most tokens, MoE training typically adds an auxiliary loss (Fedus et al., 2022):

$$\mathcal{L}_{\text{aux}} = \alpha \cdot N \cdot \sum_{i=1}^N f_i \cdot P_i, \quad (3.3)$$

where f_i is the fraction of tokens routed to expert i , P_i is the average routing probability for expert i , and α is a weighting coefficient. This loss encourages uniform expert utilization but introduces a hyperparameter that needs tuning.

Independent Routing. In MoE with independent routing, a router r_l at layer l has its own learnable \mathbf{W}_l parameters. We call this *independent routing*.

Expert Path. Let $[N] = \{1, \dots, N\}$, data follow distribution $\mathbf{x} \sim \mathcal{D}$, and E_l be a random variable of the expert selection at layer l . Denote expert selections across L layers as $\mathbf{E} = (E_1, \dots, E_L)$, called an *expert path*, which is a random variable taking values in $[N]^L$. Each E_l follows a categorical distribution over N experts: $E_l | \mathbf{x}_l \sim \text{Categorical}[\text{softmax}(\mathbf{W}_l \mathbf{x}_l)]$. Let $\mathbf{e} = (e_1, \dots, e_L)$ be a specific realization of \mathbf{E} . To quantify the *effective size of the expert path space* utilized by the MoE network, we consider the entropy on the marginal distribution of expert paths over the data distribution \mathcal{D} .

Routing Entropy. Let $P_\pi(\mathbf{e})$ denote the marginal probability of observing a particular expert path \mathbf{e} over the data distribution \mathcal{D} , defined as $P_\pi(\mathbf{e}) = \mathbb{E}_{\mathbf{x} \sim \mathcal{D}} [P(\mathbf{e} | \mathbf{x})] = \mathbb{E}_{\mathbf{x} \sim \mathcal{D}} [P(E_1 = e_1, \dots, E_L = e_L | \mathbf{x})]$. The *routing entropy* is then defined as the Shannon entropy on this marginal distribution of expert paths over the data distribution \mathcal{D} :

$$H(\mathbf{E}) = H(E_1, \dots, E_L) = - \sum_{\mathbf{e} \in [N]^L} P_\pi(\mathbf{e}) \log P_\pi(\mathbf{e}). \quad (3.4)$$

A higher $H(\mathbf{E})$ indicates that the model utilizes a more diverse set of expert combinations across the data. Computationally, the marginal distribution is intractable, thus in practice we compute an empirical routing entropy on finite data.

Expert Path for Independent Routing. For independent routing each E_l follows a categorical distribution over N experts: $E_l | \mathbf{x}_l \sim \text{Categorical}[\text{softmax}(\mathbf{W}_l \mathbf{x}_l)]$, where all \mathbf{W}_l are considered to be independent matrices as every layer has its own learnable parameters.

3.2 PathMoE: Block-wise Parameter Shared Routing

PathMoE Routing. Compared to *independent routing*, **PathMoE** shares router parameters across blocks of consecutive layers. Given L MoE layers and block size B , we partition layers into $\lceil L/B \rceil$ blocks. All layers within a block share a single router:

$$r_l = r_{\text{shared}}^{(\lceil l/B \rceil)}, \quad \forall l \in \{1, \dots, L\}. \quad (3.5)$$

Expert Path for PathMoE. For **PathMoE** routing, each E_l still follows a categorical distribution over N experts. However, for any layer l' in the same block $b = \lceil l'/B \rceil$ we have $E_{l'} | \mathbf{x}_{l'} \sim \text{Categorical}[\text{softmax}(\mathbf{W}_b \mathbf{x}_{l'})]$, where \mathbf{W}_b from different blocks are independent matrices.

3.3 Intuition behind PathMoE

Below, we provide an informal approximation of routing entropy to illustrate the intuition behind why **PathMoE** routing may reduce the effective size of the expert path space compared to independent routing.² Subsequently, we compute *empirical* routing entropy and observe that it is indeed lower for **PathMoE** than for independent routing, offering a potential explanation for the improved optimization of **PathMoE**.

²Note that: (i) in the worst case, **PathMoE** can degenerate to uniform expert routing (e.g. $\mathbf{W}_b = 0$); (ii) in the best case, independent routing can learn the same \mathbf{W}_l within the same block.

Using the chain rule of entropy, the routing entropy can be decomposed and further approximated using the first-order Markov dependency (meaningful approximation in residual networks):

$$H(\mathbf{E}) = \sum_{l=1}^L H(E_l | E_1 \dots E_{l-1}) \approx \sum_{l=1}^L H(E_l | E_{l-1}).$$

Let \mathcal{S} be the set of layer indices that start a new block, $H_{\text{indep}}(\mathbf{E})$ be the independent routing entropy and $H_{\text{PathMoE}}(\mathbf{E})$ be the **PathMoE** routing entropy. Then

$$\begin{aligned} \Delta H &= H_{\text{indep}}(\mathbf{E}) - H_{\text{PathMoE}}(\mathbf{E}) \\ &\approx \sum_{l \notin \mathcal{S}} [H_{\text{indep}}(E_l | E_{l-1}) - H_{\text{PathMoE}}(E_l | E_{l-1})]. \end{aligned}$$

Using the definition of conditional entropy $H(E_l | E_{l-1}) = H(E_l) - I(E_l; E_{l-1})$, where $I(E_l; E_{l-1})$ is the mutual information between consecutive layers, we have:³

$$\Delta H \approx \sum_{l \notin \mathcal{S}} [I_{\text{PathMoE}}(E_l; E_{l-1}) - I_{\text{indep}}(E_l; E_{l-1})].$$

Given the specific representations \mathbf{x}_l and \mathbf{x}_{l-1} , the routing decisions are sampled independently via the stochastic mechanism:

$$P(E_l, E_{l-1} | \mathbf{x}_l, \mathbf{x}_{l-1}) = P(E_l | \mathbf{x}_l)P(E_{l-1} | \mathbf{x}_{l-1}).$$

Let $p_k^{(l)}(\mathbf{x}_l) = P(E_l = k | \mathbf{x}_l)$ be the probability function for expert k . The marginal joint distribution is defined as:

$$P(E_l = i, E_{l-1} = j) = \mathbb{E}_{\mathbf{x} \sim \mathcal{D}} [p_i^{(l)}(\mathbf{x}_l) \cdot p_j^{(l-1)}(\mathbf{x}_{l-1})].$$

Then the layers are independent only if the routing probabilities are uncorrelated across the data.

Independent Routing. Given that (i) router parameters \mathbf{W}_l and \mathbf{W}_{l-1} are initialized independently and stay independent for some time during training; (ii) due to residual connections representations evolve slowly $\mathbf{x}_l \approx \mathbf{x}_{l-1}$; the decision boundaries of routing function at layer l are statistically orthogonal to those at layer $l-1$ across the data. Thus

$$\begin{aligned} P(E_l = i, E_{l-1} = j) &\approx P(E_l = i)P(E_{l-1} = j) \\ &= \mathbb{E}_{\mathbf{x} \sim \mathcal{D}} [p_i^{(l)}(\mathbf{x}_l)] \mathbb{E}_{\mathbf{x} \sim \mathcal{D}} [p_j^{(l-1)}(\mathbf{x}_{l-1})] \\ &\implies I_{\text{indep}}(E_l; E_{l-1}) \approx 0. \end{aligned}$$

PathMoE Routing. As layers $l, l-1$ are within a shared block, the router parameters are identical $\mathbf{W}_l = \mathbf{W}_{l-1}$. Due to residual connections, representations evolve slowly $\mathbf{x}_l \approx \mathbf{x}_{l-1}$, thus routing probability functions are close: $p_k^{(l)}(\mathbf{x}_l) \approx p_k^{(l-1)}(\mathbf{x}_{l-1}) \triangleq \phi_k(\mathbf{x}_l)$. Then the joint probability of selecting the same expert k at both layers:

$$P(E_l = k, E_{l-1} = k) \approx \mathbb{E}_{\mathbf{x} \sim \mathcal{D}} [\phi_k(\mathbf{x}_l)^2].$$

By Jensen's inequality, since $f(z) = z^2$ is strictly convex and the routing probability $\phi_k(\mathbf{x}_l)$ varies across the data distribution, we get that E_l and E_{l-1} are correlated and this correlation is concentrated on the diagonal:

$$\begin{aligned} \mathbb{E}_{\mathbf{x} \sim \mathcal{D}} [\phi_k(\mathbf{x}_l)^2] &> (\mathbb{E}_{\mathbf{x} \sim \mathcal{D}} [\phi_k(\mathbf{x}_l)])^2 \\ P(E_l = k, E_{l-1} = k) &> P(E_l = k) \cdot P(E_{l-1} = k) \\ \implies P(E_l, E_{l-1}) &\neq P(E_l) \cdot P(E_{l-1}) \\ \implies I_{\text{PathMoE}}(E_l; E_{l-1}) &\gg 0. \end{aligned}$$

Given $I_{\text{PathMoE}}(E_l; E_{l-1}) \gg I_{\text{indep}}(E_l; E_{l-1}) \approx 0$, we obtain $\Delta H > 0$. This shows that **PathMoE** may introduce strong inter-layer correlations for the marginal distribution of expert paths over the data distribution \mathcal{D} , significantly constraining the effective expert path space.

³Every entropy is defined on the marginal distribution of the corresponding random variable over the data distribution \mathcal{D} .

Table 1 Main results on comparison with baselines on Fineweb-100B with 0.9B total / 0.37B active MoE architecture. Throughput is reported per GPU and memory reports peak active GPU memory.

Routing	ARC-E	BoolQ	HSwag	LAMBADA	OBQA	PIQA	SocIQa	WinoGr.	Avg.	PPL	Throughput (k tok/s/GPU)	Memory (GiB)
<i>Independent Routing</i>												
Indep-MoE	44.57	56.45	45.99	46.19	29.80	66.87	38.84	51.54	47.53	12.91	55.21	66.94
Rand-MoE	40.49	61.10	37.95	38.83	28.20	64.47	38.89	50.99	45.12	16.14	75.17	47.49
X-MoE	43.27	60.55	46.26	45.22	32.20	67.63	39.61	52.80	48.44	13.21	56.37	67.06
<i>Recurrent Routing</i>												
Recurrent-MoE	44.07	54.50	46.05	47.12	30.80	67.74	38.79	53.67	47.84	12.92	54.65	69.26
<i>Path-Constrained Routing</i>												
MonoB8-MoE	42.55	57.80	46.36	46.73	31.20	65.67	37.56	54.06	47.74	13.34	56.53	62.86
LowRank-MoE	44.36	59.97	46.33	46.11	31.80	66.65	39.20	52.96	48.42	12.98	53.84	66.96
PathMoE	45.50	55.44	47.82	47.89	32.40	66.21	38.49	53.43	48.40	12.92	55.71	66.74
PathB8-MoE	43.73	59.97	46.65	46.92	31.40	66.81	40.69	54.93	48.89	12.53	55.20	66.94
PathB4-MoE	44.70	60.40	47.95	49.45	31.60	66.32	40.94	55.64	49.62	12.29	55.67	66.83

Empirical Routing Entropy. We compute empirical routing entropy over ~ 7 M tokens for both independent routing and PathMoE ($B = 4$) routing, using a network with $L = 24$ layers and $N = 16$ experts. PathMoE achieves an empirical entropy of 21.14 bits, while independent routing yields 22.20 bits—a 1-bit reduction that halves the effective path space. Smaller routing entropy for PathMoE means tokens concentrate into fewer expert paths, so each path receives more training signal—improving sample efficiency. As a result, in Section 7 we show that average correlation between consecutive layers is 85.6% for PathMoE while it is 62% for independent routing. Stronger inter-layer correlations between expert selections in PathMoE mean experts can specialize knowing what inputs to expect from coordinated predecessors, rather than handling arbitrary representations.⁴

Together, these properties offer an explanation why PathMoE would yield faster learning, more robust specialization, and graceful degradation under perturbations compared to independent routing—behavior we validate empirically in Section 7.

4 Experiments

4.1 Experimental Setup

We train and evaluate PathMoE based on the Transformer architecture. Model hyperparameter settings closely follow Qiu et al. (2024).

Training Details. Our main experiments use a 0.9B parameter model (0.37B active) with 16 experts and top-4 routing, trained on Fineweb-100B Penedo et al. (2024) for 400k steps using the Llama 2 tokenizer. We remove load balancing loss for PathMoE variants but keep weight $\alpha = 0.01$ for all other models (see discussion in Section 4.3). Full hyperparameters are given in Appendix B.

4.2 Performance Comparison

Baseline Methods. We compare against three categories of routing approaches.

Independent routing methods make routing decisions without cross-layer coordination. **Indep-MoE** employs independent routers at each layer, representing the standard MoE approach. **Rand-MoE** uses randomly initialized routers that are frozen during training, providing a lower bound on learned routing. **X-MoE** Chi et al. (2022) routes tokens on a low-dimensional L2-normalized representation space with learnable temperature to prevent representation collapse.

Recurrent routing leverages historical routing information. **Recurrent-MoE** Qiu et al. (2024) uses a shared GRU where each layer’s router receives information from the previous layer’s hidden state to avoid suboptimal token-expert combinations.

⁴Detailed validation results are in Appendix A.

Path-constrained routing methods encourage tokens to follow coherent paths. We propose several approaches to constrain the expert path space: **LowRank-MoE** uses a shared base router across all layers plus a low-rank layer-specific perturbation: $r_l(\mathbf{x}) = r_{\text{shared}}(\mathbf{x}) + \mathbf{W}_l^{\text{low}}\mathbf{x}$, where $\mathbf{W}_l^{\text{low}}$ is a low-rank matrix. This encourages similar routing across layers while allowing layer-specific adaptation. For block-based methods, B_n denotes block size n ; omitting the suffix means sharing across all layers. **Mono-MoE** shares routing *decisions* within blocks, forcing each token to use the same expert within each block. **PathMoE** shares routing *parameters* within blocks, encouraging but not enforcing consistent expert selection as representations evolve.

Evaluation Tasks. We evaluate on eight downstream tasks spanning diverse capabilities: ARC-Easy (Clark et al., 2018) (science questions), BoolQ (Clark et al., 2019) (boolean questions), HellaSwag (Zellers et al., 2019) (sentence completion), LAMBADA (Paperno et al., 2016) (language modeling), OpenBookQA (Mihaylov et al., 2018) (question answering), PIQA (Bisk et al., 2020) (physical reasoning), SocialIQA (Sap et al., 2019) (social commonsense), and WinoGrande (Sakaguchi et al., 2020) (commonsense reasoning). All results report accuracy (%); OpenBookQA, PIQA, ARC-Easy, and HellaSwag use length-normalized accuracy.

Results. Table 1 shows the performance of various routing approaches (the checkpoint with the highest average accuracy from the final 5 checkpoints is selected for each model). PathB4-MoE achieves the highest average performance (49.62%) and best validation perplexity (12.29), outperforming all baselines on both metrics. PathB8-MoE and PathMoE also match or improve upon Indep-MoE’s perplexity, demonstrating that block-wise shared routing improves both language modeling and downstream task performance.

Notably, **PathMoE** variants (sharing parameters) consistently outperform MonoB8-MoE (sharing decisions), confirming that encouraging path coherence—rather than enforcing it—provides better inductive bias. See Appendix C.2 for results on DCLM-Pro dataset. Furthermore, we found that block-wise shared routing provides orthogonal benefits: applying **PathMoE** on top of X-MoE improves average accuracy from 48.44% to 48.86%, demonstrating that cross-layer coordination complements representation-based routing enhancements (see Appendix C.3). Note that the performance differences exceed the standard deviation ($\sim 0.28\%$) across checkpoint selections.

Efficiency. We also report throughput (tokens per second per GPU) and peak memory usage during training. PathB4-MoE matches or slightly exceeds Indep-MoE efficiency (55.67 vs. 55.21 k tok/s, 66.83 vs. 66.94 GiB), as the only architectural difference is sharing router parameters within blocks, which reduces the total parameter count while maintaining identical forward and backward pass computation. Methods like Recurrent-MoE and LowRank-MoE incur additional overhead due to their more complex routing mechanisms (54.65 and 53.84 k tok/s, respectively). This demonstrates that **PathMoE**’s performance gains come without sacrificing training efficiency.

4.3 Load Balancing Without Auxiliary Losses

Conventional MoE training employs auxiliary load balancing losses to prevent expert collapse (Fedus et al., 2022). We find that **PathMoE** can be trained without auxiliary losses. Figure 3 compares training dynamics of PathB4-MoE and Indep-MoE on HellaSwag and ARC-Easy, with and without load balancing losses (LBL). PathB4-MoE without LBL (dashed blue) achieves the best final accuracy on both tasks, while removing LBL from Indep-MoE leads to more erratic training dynamics. This suggests that **PathMoE** is more robust to the removal of auxiliary losses, maintaining smooth convergence regardless of the load balancing setting. See full results in Appendix C.1.

4.4 Scaling to 16B Parameters

To verify that path-constraining benefits persist at larger scales, we train 16B parameter models (16.2B total, 2.13B active) with 64 experts and top-6 routing on DCLM-Pro Zhou et al. (2024) for 200k steps using the GPT-NeoX-20B tokenizer, without load balancing loss. We additionally evaluate on MMLU (Hendrycks et al., 2020), ARC-Challenge (Clark et al., 2018), CommonsenseQA (Talmor et al., 2019), and TriviaQA (Joshi et al., 2017) (5-shot exact match). Full hyperparameters are in Appendix B.

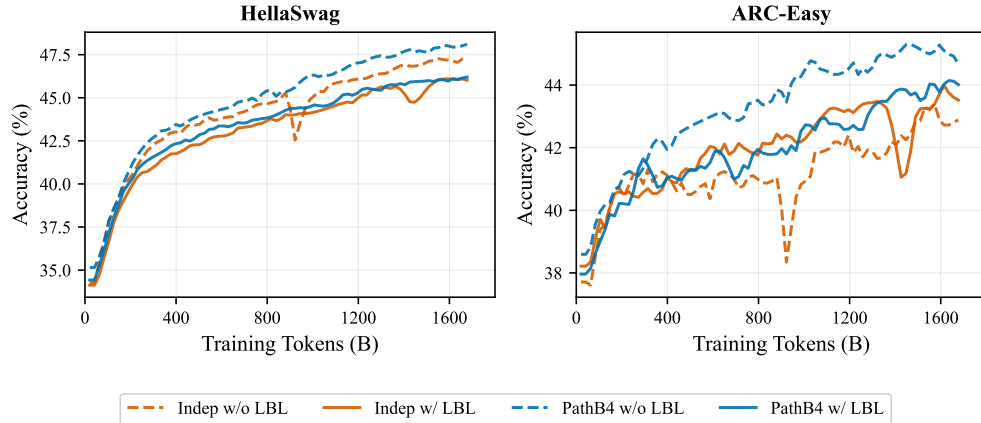


Figure 3 Training dynamics comparing PathB4-MoE and Indep-MoE with and without load balancing losses. Curves are smoothed with exponential moving average (weight=0.6) for clarity.

Table 2 shows that PathMoE wins on 10 of 12 tasks across commonsense, language, and knowledge categories, with particularly strong gains on CommonsenseQA (+5.73%), ARC-Easy (+5.09%), and OpenBookQA (+3.80%).

Table 2 16B model results on DCLM-Pro (16.2B total / 2.13B active).

Category	Task	Indep-MoE	PathMoE
<i>Commonsense</i>	WinoGrande	56.12	57.93
	PIQA	68.99	71.38
	SocialIQA	40.58	40.07
	CommonsenseQA	43.00	48.73
<i>Language</i>	LAMBADA	51.97	53.64
	HellaSwag	63.22	63.32
	BoolQ	63.06	64.01
<i>Knowledge</i>	OpenBookQA	35.80	39.60
	ARC-Easy	63.43	68.52
	ARC-Challenge	37.29	40.10
	TriviaQA	21.91	21.18
	MMLU	35.27	35.64
Average		48.39	50.34

5 Emergent Expert Path Structure

Beyond performance gains, PathMoE reveals interpretable structure in how tokens are processed. We find that expert paths are not arbitrary computational routes, but develop meaningful specializations: tokens following the same path naturally cluster by linguistic function—punctuation, named entities, temporal expressions, and other categories each tend to follow distinct paths through the network. This section examines this emergent structure: the distribution of paths (Section 5.1), the relationship between path concentration and performance (Section 5.2), and the token specialization patterns that arise (Section 5.3).

5.1 Expert Path Distribution

For each expert path \mathbf{e} we can define its *frequency* $\text{freq}(\mathbf{e})$ as the proportion of input tokens x with representations $(\mathbf{x}_1, \dots, \mathbf{x}_L)$ across layers that follow the path \mathbf{e} :

$$\text{freq}(\mathbf{e}) = \frac{|\{x : \pi(\mathbf{x}_1, \dots, \mathbf{x}_L) = \mathbf{e}\}|}{|\{x\}|}. \quad (5.1)$$

To visualize how tokens are distributed across paths, we sort paths by frequency and compute the *cumulative token coverage*: the fraction of tokens covered by the top- K most frequent paths.

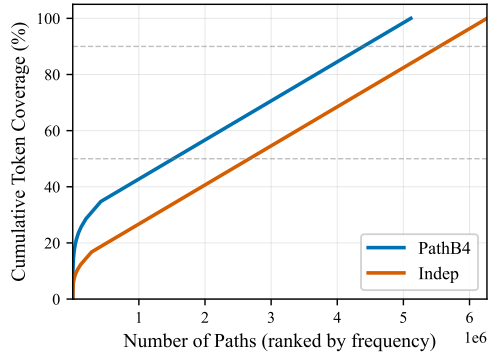


Figure 4 Cumulative token coverage as a function of the number of paths.

We analyze the empirical distribution of expert paths that emerge from **PathMoE**. **Figure 4** compares the cumulative token coverage between PathB4-MoE and Indep-MoE. We observe that PathB4-MoE concentrates tokens into fewer paths compared to Indep-MoE, with the top paths covering a larger fraction of tokens. This concentration reflects the block-wise shared routing, which encourages tokens to follow consistent paths through the network.

5.2 Expert Path Concentration

To understand the relationship between path concentration and model performance, we evaluate models with different levels of path restriction. Notably, the dominant paths emerge very early in training: we train PathB8-MoE for only 5k steps (1.25% of total training), save a checkpoint, and identify the most frequent paths at this early stage. We then continue training with routing restricted to these top-10, top-100, or top-500 paths. **Table 3** shows that restricting to only 10 paths significantly degrades performance (46.22%), 100 paths recovers most of the performance (48.18%), and 500 paths performs comparably to unrestricted routing (48.86% vs 48.71%). This suggests the model naturally concentrates on a moderate number of specialized paths.

Table 3 Effect of expert path constraints on model performance.

# Paths	ARC-E	BoolQ	HSwag	LAMBADA	OBQA	PIQA	SocIQa	WinoGr.	Avg.
10	40.45	59.54	39.34	40.87	30.40	66.81	37.82	54.54	46.22
100	43.81	56.79	47.04	45.10	30.80	67.46	40.23	54.22	48.18
500	44.74	59.42	48.24	47.58	31.20	66.00	39.97	53.75	48.86
All	44.82	56.48	47.76	46.42	31.60	66.76	39.41	56.43	48.71

5.3 Expert Path Token Specialization

Figure 5 reveals that expert paths develop distinct linguistic specializations without any supervision. Some paths predominantly process punctuation, others handle person names or speech verbs (“said”, “explained”), and yet others specialize in temporal expressions or function words. This clustering by linguistic function

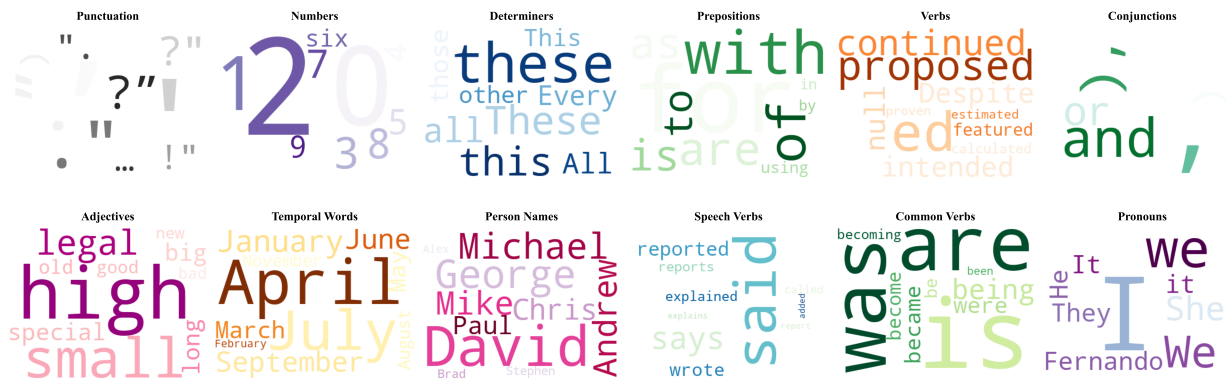


Figure 5 Token specialization of representative expert paths. Each word cloud shows the most frequent tokens processed by a path specialized for that linguistic category.

emerges purely from the language modeling objective: the model learns to route syntactically or semantically similar tokens through shared computational pathways. Notably, this specialization is also observed in Indep-MoE, suggesting it is a general property of MoE routing rather than specific to our method. However, PathMoE produces more concentrated token clusters within each path. Thus we observe an interpretable routing structure where each expert path develops expertise for particular linguistic phenomena.

6 Ablation Studies

Top- k Routing Analysis. We investigate the effect of the top- k routing parameter across values of 1, 2, 4, 8, and 16. Figure 6(a) shows that top-2 routing achieves the best average accuracy (49.99%), consistent with Mixtral Jiang et al. (2024). Performance degrades at both extremes: $k=1$ suffers from training instability and limited capacity, while $k=16$ dilutes expert contributions—both yield similar accuracy ($\sim 45.7\%$). The sweet spot at $k=2$ provides sufficient capacity while maintaining specialization pressure, with particularly strong gains on LAMBADA (+10.3%) and HellaSwag (+8.1%) compared to $k=1$.

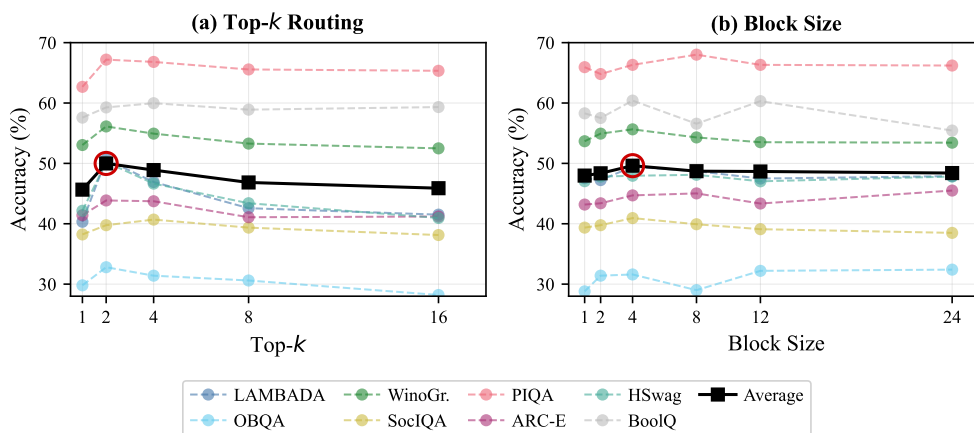


Figure 6 Ablation studies on routing hyperparameters. (a) Effect of top- k routing: top-2 achieves best average accuracy (circled). (b) Effect of block size: B4 achieves best average accuracy (circled). Dashed lines show individual benchmarks; solid black line shows the average.

Block Size Analysis. We investigate the effect of block size across values of 1, 2, 4, 8, 12, and 24 layers. Block size controls the trade-off between routing flexibility and cross-layer coordination: small blocks (B1, B2) provide insufficient coordination as layers learn nearly independently, while large blocks (B12, B24)

over-constrain the router to handle representations that change substantially across layers. Figure 6(b) confirms that intermediate sizes work best: B4 achieves the highest average accuracy (49.62%). We observe task-dependent preferences—language modeling and commonsense tasks peak at B4, physical reasoning at B8, and knowledge-intensive tasks at B24—suggesting that optimal block size may vary by domain.

7 Understanding PathMoE: Routing Consistency and Robustness

Beyond performance gains, understanding *why* PathMoE works can guide future MoE design. We examine two key properties: cross-layer routing consistency and robustness to perturbations.

7.1 Cross-Layer Routing Consistency

Since expert indices are arbitrary across layers (expert 0 at layer l has no inherent correspondence to expert 0 at layer $l + 1$), we first align indices by finding permutations that maximize cross-layer agreement. We then examine two complementary metrics. **Path consistency** measures expert reuse: we compute the average Jaccard similarity between expert sets at consecutive layers. **Sustained engagement** measures how long a token continues using a given aligned expert: we count runs of consecutive layers and report the fraction lasting $\geq X$ layers.

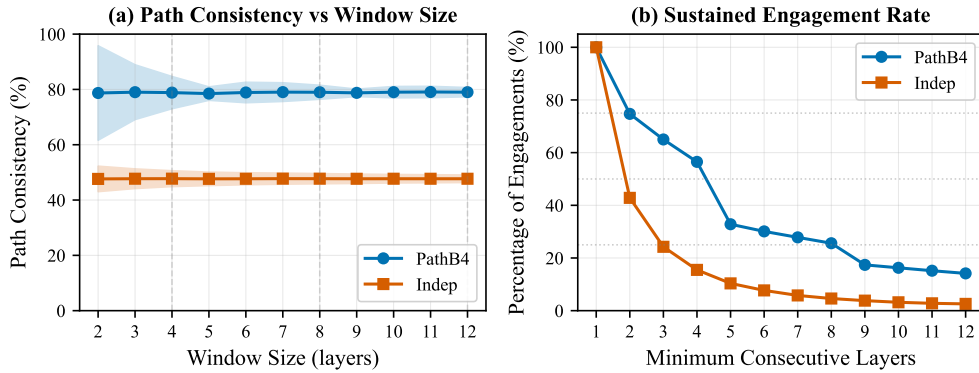


Figure 7 Cross-layer routing consistency. (a) Path consistency versus window size. (b) Sustained engagement versus minimum consecutive layers.

Figure 7(a) shows that PathMoE maintains consistently higher path consistency ($\sim 79\%$) compared to Indep-MoE ($\sim 48\%$) across all window sizes from 2 to 12 layers. This gap persists even at non-block-aligned windows (3, 5, 7 layers), confirming the benefit stems from the architecture rather than block boundaries. Panel (b) measures how long tokens continue using the same expert, where PathMoE produces substantially more sustained engagements.

7.2 Expert Specialization and Routing Robustness

We examine the specialization-robustness trade-off to check whether PathMoE’s routing creates brittle dependencies.

Routing Specialization. We measure specialization via routing entropy: for each token, we compute the entropy of its expert usage distribution across all layers, where lower entropy indicates more concentrated (specialized) routing. Figure 8(a) shows that PathB4-MoE achieves consistently lower entropy than Indep-MoE across all layers, with 11% lower entropy at the final layer.

Routing Robustness. We test robustness by randomly permuting expert indices at each layer with probability p and measuring perplexity degradation. Figure 8(b) shows that PathMoE is dramatically more robust despite being more specialized: at full permutation, Indep-MoE degrades by 5,328% versus only 237% for PathMoE. Thus, the two methods specialize differently.

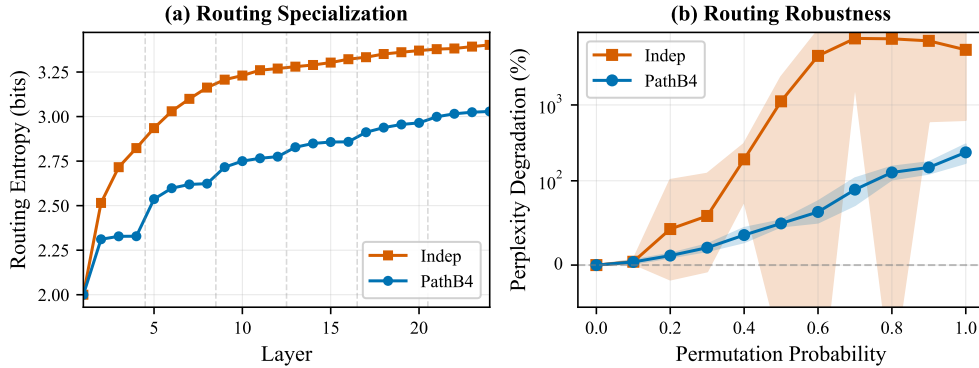


Figure 8 Routing specialization and robustness. (a) Cumulative routing entropy across layers. (b) Perplexity degradation under expert permutation.

8 Conclusion

We introduced **PathMoE**, which constrains the combinatorial expert path space by sharing router parameters within blocks of consecutive layers. This simple modification yields three key benefits: (1) consistent performance gains on downstream tasks—+2.1% average accuracy on the 0.9B model and winning 10 of 12 tasks on the 16B model—*without auxiliary load balancing losses*; (2) improved cross-layer coordination (79% vs. 48% routing consistency); (3) more specialized yet more robust routing (11% lower entropy, 22.5× more robust to perturbations).

Analysis reveals that expert paths develop interpretable linguistic specializations, with tokens clustering by function—punctuation, named entities, temporal expressions—purely from the language modeling objective. The block-wise design provides a middle ground between independent routing (too flexible, N^L paths) and fully shared routing (too rigid), encouraging path coherence while allowing adaptation across network depth.

A limitation is that block-wise sharing assumes token-choice routing; preliminary experiments show no benefit for expert-choice routing, which already achieves consistency through stable expert preferences. Future work could explore learning the expert path predictors jointly with the main model or using the expert path structure for model compression.

Impact Statement

This paper introduces an architectural modification to Mixture-of-Experts routing that improves downstream model performance, cross-layer coordination and model interpretability. By encouraging tokens to follow coherent expert paths, our approach reveals how MoE models naturally develop linguistic specializations—providing insights that could aid model understanding and debugging.

The efficiency gains from eliminating auxiliary load balancing losses and achieving better parameter utilization could reduce the computational cost of training large models. However, our work focuses on routing mechanisms rather than capability scaling, and does not introduce risks beyond those inherent to large language models research.

Acknowledgements

We thank Ronan Collobert, Yizhe Zhang, Samira Abnar, Anastasiia Filippova, Shuangfei Zhai, Russ Webb and Barry Theobald for helpful discussions and feedback.

References

- Yonatan Bisk, Rowan Zellers, Jianfeng Gao, Yejin Choi, et al. Piqa: Reasoning about physical commonsense in natural language. In *Proceedings of the AAAI conference on artificial intelligence*, volume 34, pages 7432–7439, 2020.
- Zewen Chi, Li Dong, Shaohan Huang, Damai Dai, Shuming Ma, Barun Patra, Saksham Singhal, Payal Bajaj, Xia Song, Xian-Ling Mao, et al. On the representation collapse of sparse mixture of experts. *Advances in Neural Information Processing Systems*, 35:34600–34613, 2022.
- Christopher Clark, Kenton Lee, Ming-Wei Chang, Tom Kwiatkowski, Michael Collins, and Kristina Toutanova. Boolq: Exploring the surprising difficulty of natural yes/no questions. *arXiv preprint arXiv:1905.10044*, 2019.
- Peter Clark, Isaac Cowhey, Oren Etzioni, Tushar Khot, Ashish Sabharwal, Carissa Schoenick, and Oyvind Tafjord. Think you have solved question answering? try arc, the ai2 reasoning challenge. *arXiv preprint arXiv:1803.05457*, 2018.
- Damai Dai, Li Dong, Shuming Ma, Bo Zheng, Zhifang Sui, Baobao Chang, and Furu Wei. Stablemoe: Stable routing strategy for mixture of experts. *arXiv preprint arXiv:2204.08396*, 2022.
- Damai Dai, Chengqi Deng, Chenggang Zhao, RX Xu, Huazuo Gao, Deli Chen, Jiashi Li, Wangding Zeng, Xingkai Yu, Yu Wu, et al. Deepseekmoe: Towards ultimate expert specialization in mixture-of-experts language models. *arXiv preprint arXiv:2401.06066*, 2024.
- Nan Du, Yanping Huang, Andrew M Dai, Simon Tong, Dmitry Lepikhin, Yuanzhong Xu, Maxim Krikun, Yanqi Zhou, Adams Wei Yu, Orhan Firat, et al. Glam: Efficient scaling of language models with mixture-of-experts. In *International conference on machine learning*, pages 5547–5569. PMLR, 2022.
- William Fedus, Barret Zoph, and Noam Shazeer. Switch transformers: Scaling to trillion parameter models with simple and efficient sparsity. *Journal of Machine Learning Research*, 23(120):1–39, 2022.
- Zijin Gu, Tatiana Likhomanenko, and Navdeep Jaitly. Omni-router: Sharing routing decisions in sparse mixture-of-experts for speech recognition. *arXiv preprint arXiv:2507.05724*, 2025.
- Dan Hendrycks, Collin Burns, Steven Basart, Andy Zou, Mantas Mazeika, Dawn Song, and Jacob Steinhardt. Measuring massive multitask language understanding. *arXiv preprint arXiv:2009.03300*, 2020.
- Jordan Hoffmann, Sebastian Borgeaud, Arthur Mensch, et al. Training compute-optimal large language models. *arXiv preprint arXiv:2203.15556*, 2022.
- Robert A Jacobs, Michael I Jordan, Steven J Nowlan, and Geoffrey E Hinton. Adaptive mixtures of local experts. *Neural computation*, 3(1):79–87, 1991.
- Albert Q Jiang, Alexandre Sablayrolles, Antoine Roux, Arthur Mensch, Blanche Savary, Chris Bamford, Devendra Singh Chaplot, Diego de las Casas, Emma Bou Hanna, Florian Bressand, et al. Mixtral of experts. *arXiv preprint arXiv:2401.04088*, 2024.
- Mandar Joshi, Eunsol Choi, Daniel S Weld, and Luke Zettlemoyer. Triviaqa: A large scale distantly supervised challenge dataset for reading comprehension. *arXiv preprint arXiv:1705.03551*, 2017.
- Dmitry Lepikhin, HyukJoong Lee, Yuanzhong Xu, Dehao Chen, Orhan Firat, Yanping Huang, Maxim Krikun, Noam Shazeer, and Zhifeng Chen. Gshard: Scaling giant models with conditional computation and automatic sharding. *arXiv preprint arXiv:2006.16668*, 2020.
- Todor Mihaylov, Peter Clark, Tushar Khot, and Ashish Sabharwal. Can a suit of armor conduct electricity? a new dataset for open book question answering. *arXiv preprint arXiv:1809.02789*, 2018.
- Denis Paperno, Germán Kruszewski, Angeliki Lazaridou, Ngoc-Quan Pham, Raffaella Bernardi, Sandro Pezzelle, Marco Baroni, Gemma Boleda, and Raquel Fernández. The lambada dataset: Word prediction requiring a broad discourse context. In *Proceedings of the 54th annual meeting of the association for computational linguistics (volume 1: Long papers)*, pages 1525–1534, 2016.
- Guilherme Penedo, Hynek Kydlíček, Anton Lozhkov, Margaret Mitchell, Colin A Raffel, Leandro Von Werra, Thomas Wolf, et al. The fineweb datasets: Decanting the web for the finest text data at scale. *Advances in Neural Information Processing Systems*, 37:30811–30849, 2024.
- Joan Puigcerver, Carlos Riquelme, Basil Mustafa, and Neil Houlsby. From sparse to soft mixtures of experts. *arXiv preprint arXiv:2308.00951*, 2023.

- Zihan Qiu, Zeyu Huang, Shuang Cheng, Yizhi Zhou, Zili Wang, Ivan Titov, and Jie Fu. Layerwise recurrent router for mixture-of-experts. *arXiv preprint arXiv:2408.06793*, 2024.
- David Raposo, Sam Ritter, Blake Richards, Timothy Lillicrap, Peter Conway Humphreys, and Adam Santoro. Mixture-of-depths: Dynamically allocating compute in transformer-based language models. *arXiv preprint arXiv:2404.02258*, 2024.
- Keisuke Sakaguchi, Ronan Le Bras, Chandra Bhagavatula, and Yejin Choi. Winogrande: An adversarial winograd schema challenge at scale. In *Proceedings of the AAAI Conference on Artificial Intelligence*, volume 34, pages 8732–8740, 2020.
- Maarten Sap, Hannah Rashkin, Derek Chen, Ronan LeBras, and Yejin Choi. Socialiqa: Commonsense reasoning about social interactions. *arXiv preprint arXiv:1904.09728*, 2019.
- Noam Shazeer, Azalia Mirhoseini, Krzysztof Maziarsz, Andy Davis, Quoc Le, Geoffrey Hinton, and Jeff Dean. Outrageously large neural networks: The sparsely-gated mixture-of-experts layer. *arXiv preprint arXiv:1701.06538*, 2017.
- Alon Talmor, Jonathan Herzig, Nicholas Lourie, and Jonathan Berant. Commonsenseqa: A question answering challenge targeting commonsense knowledge. In *Proceedings of the 2019 Conference of the North American Chapter of the Association for Computational Linguistics: Human Language Technologies, Volume 1 (Long and Short Papers)*, pages 4149–4158, 2019.
- Cheng Yang, Yang Sui, Jinqi Xiao, Lingyi Huang, Yu Gong, Yuanlin Duan, Wenqi Jia, Miao Yin, Yu Cheng, and Bo Yuan. MoE-I²: Compressing mixture of experts models through inter-expert pruning and intra-expert low-rank decomposition. *arXiv preprint arXiv:2411.01016*, 2024.
- Ted Zadouri, Ahmet Üstün, Arash Ahmadian, Beyza Ermis, Acyr Locatelli, and Sara Hooker. Pushing mixture of experts to the limit: Extremely parameter efficient moe for instruction tuning. *arXiv preprint arXiv:2309.05444*, 2023.
- Rowan Zellers, Ari Holtzman, Yonatan Bisk, Ali Farhadi, and Yejin Choi. Hellaswag: Can a machine really finish your sentence? *arXiv preprint arXiv:1905.07830*, 2019.
- Fan Zhou, Zengzhi Wang, Qian Liu, Junlong Li, and Pengfei Liu. Programming every example: Lifting pre-training data quality like experts at scale. *arXiv preprint arXiv:2409.17115*, 2024.
- Yanqi Zhou, Tao Lei, Hanxiao Liu, Nan Du, Yanping Huang, Vincent Zhao, Andrew M Dai, Quoc V Le, James Laudon, et al. Mixture-of-experts with expert choice routing. *Advances in Neural Information Processing Systems*, 35:7103–7114, 2022.

A Empirical Routing Entropy

We provide detailed empirical routing entropy computation and expert path space statistics for both independent routing and PathMoE routing from Section 3. Table 4 reports comprehensive metrics for Indep-MoE and PathB4-MoE measured on 7.18M tokens.

Table 4 Detailed empirical routing entropy computation and expert path space statistics for Indep-MoE and PathB4-MoE (block size $B = 4$) with $L = 24$ layers and $N = 16$ experts. All entropy measurements are in bits. We use evaluation data with 7.18M tokens.

Empirical Metric	PathB4-MoE	Indep-MoE
Routing entropy $H(\mathbf{E})$	21.14 bits	22.20 bits
Routing decisions correlation for consecutive layers	85.6%	62%
Unique paths observed	5,109,282	6,263,708
Effective path space $2^{H(\pi)}$	2.31×10^6	4.82×10^6

B Training Details

Table 5 summarizes the hyperparameters for both model scales.

Table 5 Training hyperparameters for 0.9B and 16B models.

Hyperparameter	0.9B Model	16B Model
<i>Model Architecture</i>		
Total parameters	0.9B	16.2B
Active parameters	0.37B	2.13B
Model dimension	1280	2048
FFN hidden dimension	768	2112
Layers	24	28
Attention heads	20	16
KV heads	4	16
Experts	16	64
Top- k routing	4	6
<i>Training</i>		
Dataset	Fineweb-100B	DCLM-Pro
Tokenizer	Llama 2 (32k)	GPT-NeoX-20B
Sequence length	4096	4096
Global batch size	1024	2048
Training steps	400k	200k
<i>Optimization</i>		
Optimizer	AdamW	AdamW
β_1, β_2	0.9, 0.95	0.9, 0.95
Weight decay	0.1	0.1
Peak learning rate	4.2×10^{-4}	2.0×10^{-4}
LR schedule	Cosine	Cosine
Warmup steps	2000	2000
Precision	BF16	BF16

The 0.9B model architecture follows Qiu et al. (2024). The 16B model architecture follows DeepSeek-MoE Dai et al. (2024) without shared experts to isolate the effect of routing changes.

C Additional Results

C.1 Results on removing load balancing loss (0.9B Model)

We provide full experimental results on keeping and removing load balancing loss (LBL) for Indep-MoE and PathB4-MoE.

Table 6 Performance comparison on Fineweb-100B dataset (0.9B total / 0.37B active).

Routing	LBL	ARC-E	BoolQ	HSwag	LAMBADA	OBQA	PIQA	SocIQA	WinoGr.	Avg.
Indep-MoE	0.01	44.57	56.45	45.99	46.19	29.80	66.87	38.84	51.54	47.53
Indep-MoE	0	43.18	58.29	47.05	47.55	28.80	65.94	39.36	53.67	47.98
PathB4-MoE	0.01	44.15	57.06	46.07	46.61	32.60	66.49	40.23	51.93	48.14
PathB4-MoE	0	44.70	60.40	47.95	49.45	31.60	66.32	40.94	55.64	49.62

C.2 Results on DCLM-Pro Dataset (0.9B Model)

We provide additional experimental results on the DCLM-Pro dataset using the 0.9B (total) parameter model. [Table 7](#) presents the performance comparison across routing methods.

Table 7 Performance comparison on DCLM-Pro dataset (0.9B total / 0.37B active).

Routing	ARC-E	BoolQ	HSwag	LAMBADA	OBQA	PIQA	SocIQA	WinoGr.	Avg.
Indep-MoE	55.18	56.27	48.19	40.73	35.80	66.70	39.46	55.96	49.79
LowRank-MoE	58.84	59.42	48.26	40.68	33.00	66.54	40.69	54.38	50.22
PathMoE	57.49	60.06	48.30	40.69	34.40	67.25	39.87	56.99	50.63
PathB8-MoE	58.16	58.20	48.26	40.35	34.40	66.65	40.33	54.38	50.09

C.3 Orthogonal Benefits with Other Routing Methods

Block-wise shared routing provides orthogonal benefits that can be combined with other routing improvements. [Table 8](#) shows the performance of applying **PathMoE** (block size 4) on top of X-MoE, which routes tokens on a low-dimensional normalized representation space. Load balancing losses are used for both models.

Table 8 Combining **PathMoE** with X-MoE on Fineweb-100B (0.9B total / 0.37B active). **PathMoE** improves X-MoE’s average accuracy (standard deviation is $\sim 0.28\%$).

Routing	ARC-E	BoolQ	HSwag	LAMB.	OBQA	PIQA	SocIQA	WinoGr.	Avg.
X-MoE	43.27	60.55	46.26	45.22	32.20	67.63	39.61	52.80	48.44
PathB4X-MoE	44.07	61.07	47.29	48.30	30.80	66.43	39.97	52.96	48.86

The improvement demonstrates that cross-layer coordination through block-wise shared routing complements representation-based routing enhancements, suggesting that **PathMoE** can be applied as a general technique on top of existing routing methods.

C.4 Token Category Definitions

For our path specialization analysis, we classify tokens into detailed linguistic categories. [Table 9](#) provides the complete list of categories used in our analysis.

Table 9 Token categories used for path specialization analysis. Each category is defined by curated word lists or morphological patterns.

Category	Type	Examples
person_names	Lexical	Andrea, Richard, Oprah, Mary, John, Elizabeth
titles_roles	Lexical	secretary, minister, commander, winner, professor, CEO
speech_verbs	Lexical	said, explained, told, asked, claimed, announced
adverbs_discourse	Lexical	especially, actually, particularly, however, therefore
adverbs_manner	Lexical	quickly, carefully, successfully, directly, properly
adverbs_time	Lexical	now, today, recently, always, sometimes, currently
adverbs_other	Pattern	Words ending in -ly not in above lists
nationalities	Lexical	American, British, Chinese, European, Japanese
temporal_words	Lexical	Monday, January, morning, year, summer, afternoon
prepositions	Lexical	in, on, at, to, for, with, by, from, about
conjunctions	Lexical	and, or, but, because, although, while, if
determiners	Lexical	the, a, an, this, that, some, every, each
pronouns	Lexical	he, she, they, it, who, someone, anybody
quantifiers	Lexical	all, many, most, million, percent, several
common_verbs	Lexical	is, have, go, make, take, know, said, get
verbs	Pattern	Words ending in -ing or -ed (running, created)
adjectives	Lexical	good, new, important, political, economic, public
proper_nouns	Pattern	Capitalized words not in name list
abstract_nouns	Pattern	Words ending in -tion/-sion/-ness/-ment
agent_nouns	Pattern	Words ending in -er/-or (player, actor)
numbers	Pattern	Numeric digits (1, 2, 100, 2024)
ordinals	Pattern	Numeric ordinals (1st, 2nd, 3rd)
punctuation	Pattern	Punctuation marks (. , ! ? ; : ' " ()